ACS APPLIED MATERIALS & INTERFACES

Research Article

www.acsami.org

Soft Matter Beats Hard Matter: Rupturing of Thin Metallic Films Induced by Mass Transport in Photosensitive Polymer Films

Nataraja Sekhar Yadavalli, Felix Linde, Alexey Kopyshev, and Svetlana Santer*

Department of Experimental Physics, Institute for Physics and Astronomy, University of Potsdam, Karl-Liebknecht Strasse 24/25, 14476 Potsdam, Germany

ABSTRACT: The interface between thin films of metal and polymer materials play a significant role in modern flexible microelectronics *viz.*, metal contacts on polymer substrates, printed electronics and prosthetic devices. The major emphasis in metal−polymer interface is on studying how the externally applied stress in the polymer substrate leads to the deformation and cracks in metal film and vice versa. Usually, the deformation process involves strains varying over large lateral dimensions because of excessive stress at local imperfections. Here we show that the seemingly random phenomena at macroscopic scales can be rendered rather controllable at submicrometer length scales. Recently, we have created a metal−polymer interface system with strains varying over periods of several hundred nanometers. This was achieved by exploiting the formation of surface relief grating (SRG) within the azobenzene containing photosensitive polymer film upon irradiation with light interference pattern. Up to a thickness of 60 nm, the adsorbed metal film adapts neatly to the forming relief, until it ultimately ruptures into an array of stripes by formation of highly regular and uniform cracks along the maxima and minima of the polymer topography. This surprising phenomenon has far-reaching implications. This is the first time a direct probe is available to estimate the forces emerging in SRG formation in glassy polymers. Furthermore, crack formation in thin metal films can be studied literally in slow motion, which could lead to substantial improvements in the design process of flexible electronics. Finally, cracks are produced uniformly and at high density, contrary to common sense. This could offer new strategies for precise nanofabrication procedures mechanical in character.

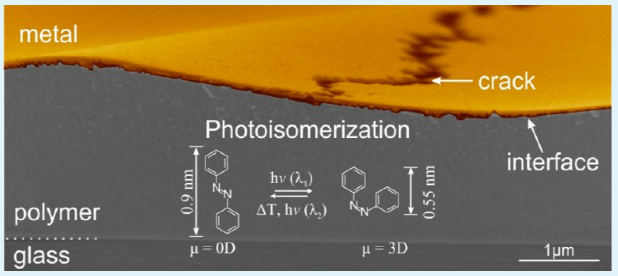

KEYWORDS: *metal/polymer interface, rupturing of metal film, forces generated during surface relief grating formation, in situ atomic force microscopy, azobenzene, two beam interferometry*

INTRODUCTION

The phenomenon of surface relief grating (SRG) formation in thin azo-benzene containing photosensitive polymer films is known for more than 20 years.[1,2] In this process, irradiation with light interference patterns causes the topography of the photosensitive polymer to follow the intensity distribution of the impinging light beam. This is interesting, as a local change of the molecular properties of the azo-benzene molecules occurs, consisting of a photoisomerisation reaction from trans to cis,[3−10] but in turn also the structure of the whole polymer matrix changes.[11−21] This initiation of material flow by absorption of light even occurs at room temperature in air, i.e., in a glassy state when the polymer is supposed to be solidlike. The optomechanical deformation of the azo-benzene polymer layers is not only restricted to a thin film geometry, but also takes place in a macroscopic piece of polymeric material. This has, for instance, inspired the construction of light-driven artificial muscles[22,23] and light-powered electrical switch based on cargo-lifting azobenzene monolayers.[24] Intuitively, one may expect fairly strong local forces that are able to deform an otherwise glassy film.

Viscoplastic theory, for instance, would imply that in order to cause polymer mass transport well below the glass transition temperature, the light-induced stress within the polymer must be far above the yield point of the azobenzene polymer.[25] A theoretical account of SRG formation in noncovalently attached films proposed by Saphianikova et al. gives an estimation of about 100 MPa for the striction stress that appears under homogeneous illumination,[26−28] far above the yield stress for conventional polymers uniaxially stretched at small strain rates.[29]

In fact, the forces are so strong that covalent bonds can be broken. Recent research on photosensitive polymer brushes reveals that during SRG formation, covalently tethered polymer chains (decorated with azo-benzene containing side chains) are ruptured locally from the areas of receding polymer material.[30,31] The average strength of C−C covalent bond is about 2 nN, the corresponding stress needed for the scission of a polymer chain in a brush of grafting density 1 nm^{-2} (one chain per nm^2) should therefore be about 2 GPa. A similar value was inferred in the group of Prof. Barrett in a different context, using a sophisticated experimental setup where the polymer

Received: February 22, 2013
Accepted: July 30, 2013
Published: July 30, 2013

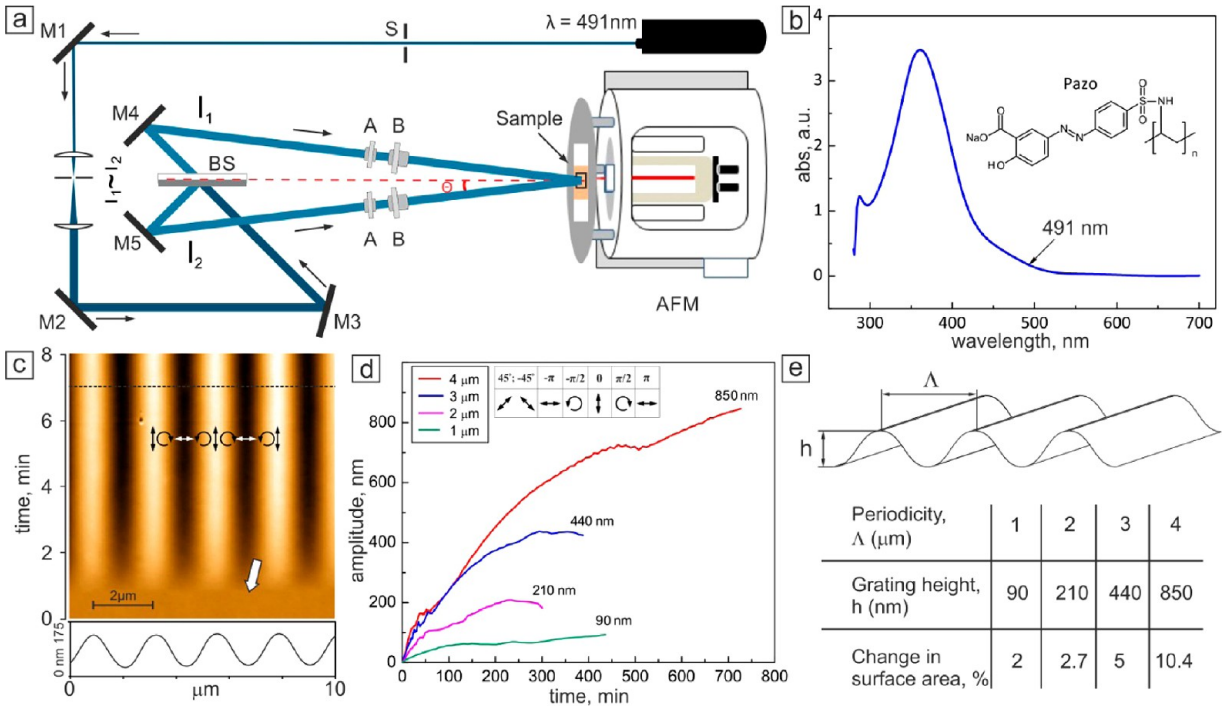

Figure 1. (a) Scheme of the experimental setup combining two beam interferometry with AFM. The letters designate the shutter (S), mirrors (M), beam splitter (BS), $\lambda/2$ plate (A), polarizer (B), and beam intensity (I), respectively. The laser beam of a diode pumped solid state laser (50 mW input intensity, λ = 491 nm) is expanded and collimated with a pair of focusing and collimating lenses and a pinhole. The collimated beam is split into two halves with equal intensities and the two beams are aligned to interfere at the sample positioned in the AFM for in situ measurement. The grating periodicity, $\Lambda = \lambda/(2\sin\theta)$, is controlled by the angle θ. (b) chemical structure and absorption spectrum of the PAZO photosensitive polymer. (c) AFM micrograph of SRG growth recorded in situ during scanning from bottom to top with the interference pattern distribution is showed on grating topography. (d) Dependence of the height of the topography grating on irradiation time for four different periodicities: 1, 2, 3, and 4 μm. The insert shows the variation of the polarization along the grating vector (perpendicular to the grating formed). (e) Table summarizing the maximal grating height and corresponding change in surface area of the polymer surface for different periodicities of the SRG.

film was put under uniaxial stress and the change in thickness of the film was detected during irradiation with UV light as a function of applied stress. It was found that up to a level of 1.2 GPa the photoisomerization of the azobenzene groups still leads to a noticeable change in polymer thickness.[32]

The above-mentioned estimations indicate that forces inscribing a topographical pattern into a thin film should be fairly large, but are hard to assess directly. In the present work, we probe the strength of the material transport by depositing nanometer-thick gold layers on top of photosensitive polymer films. The gold film is meant to be a probe, the deformation of which along with the topographical changes in the polymer could be used to characterize the magnitude of the forces originating from the optically induced phase transitions.

MATERIALS AND METHODS

Sample Preparation. The photosensitive polymer (poly{1-[4-(3-carboxy-4-hydroxyphenylazo)benzenesulfonamido]-1,2-ethanediyl,sodiumsalt}) (PAZO) with molecular weight of M_n = 1.4 × 10^4 g/mol was purchased from Sigma-Aldrich. The films were prepared by spin-casting on thin glass surface (thickness of 130 - 160 μm from Carl Roth GmbH, Germany) 95% methoxyethanol and 5% ethyleneglycol solution at a concentration of 250 mg/mL at 11 000 rpm for 1 min.[33] The gold films of a thickness varying between 5 to 60 nm were deposited on the polymer layers by a metal evaporation process (Leybold Oerlikon Univex 350) at a deposition rate of 0.25 nm/sec.

In Situ Interferometric AFM Setup. To inscribe the surface relief grating, we used a continuous wave diode pumped solid state laser operating in a single longitudinal mode with 50 mW output power at wavelength of 491 nm (Cobalt Calypso). The laser beam was spatially expanded and collimated with a pair of focusing and collimating lenses and a pinhole. The collimated beam was split into two halves with equal intensities using a nonpolarizing beam splitter and the two beams were aligned to interfere at sample positioned in AFM for in situ measurements of grating formation. The AFM measurements were conducted in tapping mode using Pico equipment (Agilent, USA) and cantilevers with resonance frequency of ~130 kHz and the force constant of ~27 N/m (Nanosensors). The AFM scan speed was 1 Hz, so that each subsequent micrograph was recorded with a time shift of 512 s. The grating periodicity [$\Lambda = \lambda/(2\sin\theta)$] was controlled by the angle θ (see Figure 1a). The linear polarizations of the two interfered beams (I_1 and I_2) were fixed at ±45°, respectively, resulting in a polarization interference pattern. We choose this polarization combination of ±45° because during irradiation with this interference pattern one achieves the largest change in SRG height and thus in strain.[34]

RESULTS AND DISCUSSION

To record the process of SRG formation in situ during irradiation and thus to gain insight into the kinetics of mass transport and the related deformation of the adsorbed gold layer, we designed a special setup combining the optical part for the generation of interference patterns and the AFM for

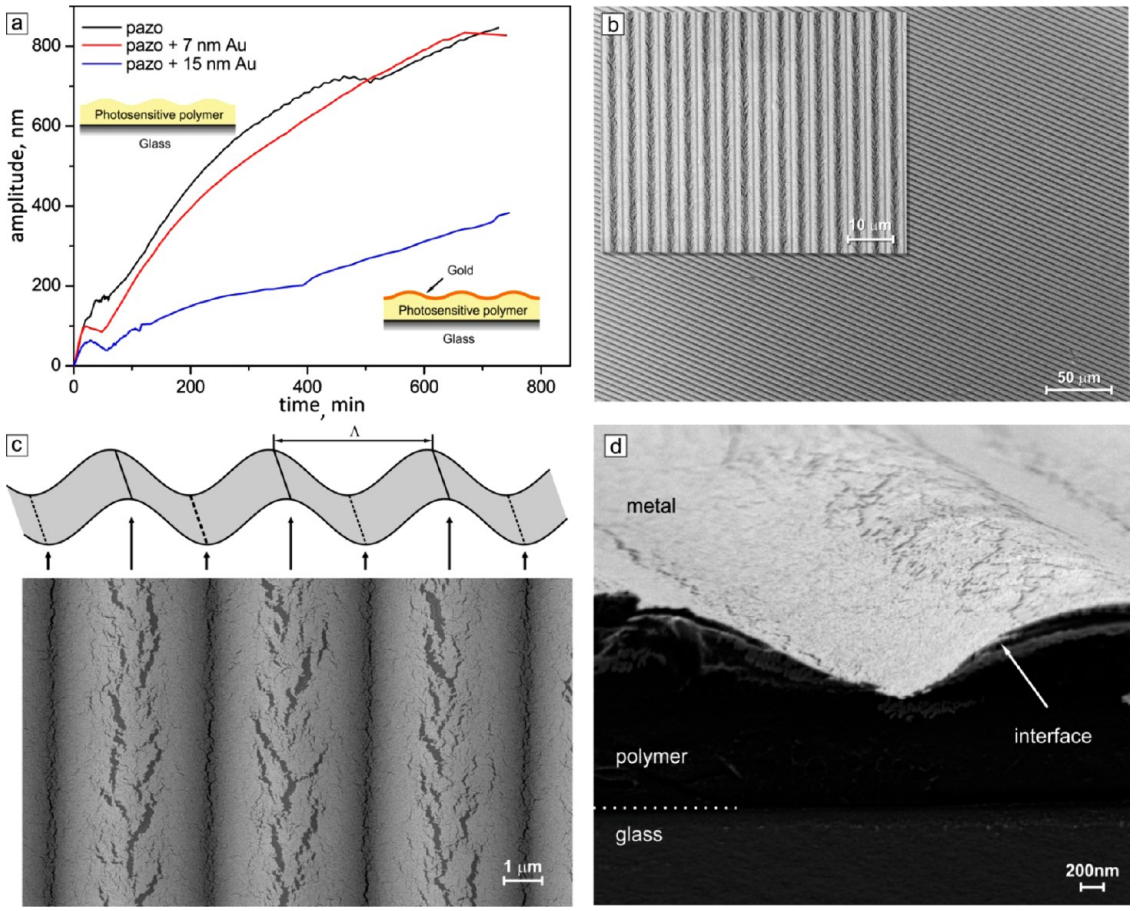

Figure 2. (a) Dependence of the grating height on irradiation time for the polymer without (black curve), and with a gold layer on top. The thin layer of 7 nm gold (red line) does not influence the SRG growth. At a thickness of roughly 15 nm (blue line), the rigid film slows the kinetics of grating formation. The insets show the scheme of the measured samples. (b–d) SEM micrographs of the ruptured gold layer. In c, a scheme of the SRG is inserted with indications of the location of the crack positions.

acquiring changes in topography during irradiation (Figure 1a). Using the in situ inteferometric AFM setup, we studied the evolution of the grating formation for different periodicities (period lengths) of the interference patterns (1, 2, 3, and 4 μm), see Figure 1d. During scanning from bottom to top at a certain point (marked by the arrow in Figure 1c), we switch on the irradiation. This results in an immediate response of the polymer topography. From the kinetics of the grating formation (Figure 1d), it can be inferred that the height of the stripes formed increases gradually with irradiation time and the stripe height grows with increasing periodicity. In situ measurements are continued until the growth of the grating height (the vertical difference between grating maxima and minima) saturates or when the grating growth rate is negligible. It is observed that the maximum height of 850 nm (around 85% of total polymer film thickness) was achieved at a periodicity of 4 μm after 12 h of irradiation

With respect to the deforming metal it is most important to track the change in surface area during grating formation, as it gives us the change in strain of the adsorbed film. To calculate the change in the surface area, we assume sinusoidal profile of the SRG:$z(x) = A_o\sin((2\pi x)/(\Lambda))$, where A_o, Λ are half of the grating height and the periodicity of the SRG; we can then calculate the arc length s for the one period as

$$s = \int_0^{\Lambda} \sqrt{1 + [z'(x)]^2}\, dx$$

$$= \int_0^{\Lambda} \sqrt{1 + A_0^2 \frac{4\pi^2}{\Lambda^2}\left(\cos\frac{2\pi x}{\Lambda}\right)^2}\, dx$$

By solving this integral numerically, we have found that a maximum change in surface area of ca. 10% occurs for a periodicity of 4 μm (Figure 1e). We consequently chose this combination of the SRG parameter, i.e., Λ = 4 μm, and the height, h = 850 nm, for the study of metal deformation.

With a gold layer on top of the polymer, the maximally attainable stripe height reduces for the thicker gold layer starting from 15 nm (Figure 2). In this case the change in the surface area is 2.4%. In the case of thinner layer constrain of rigid metal layer does not influence the change in polymer topography, as it is seen from the kinetic of the grating growth with, h_{Au} = 7 nm, and without metal (Figure 2a).

Examining the gold film with scanning electron microscopy reveals an interesting phenomenon: the gold layer is ruptured all over the irradiation area (Figure 2b). This is quite surprising as it shows that the forces induced during polymer film deformation can do quite an amount of work per unit volume. The rupturing is homogeneous along the stripes and appears twice a period, i.e. at the topography maxima and minima (Figure 2c, d). The shape and the size of the formed cracks differ depending on their position on the SRG (Figure 2c).

dx.doi.org/10.1021/am400682w | ACS Appl. Mater. Interfaces 2013, 5, 7743–7747

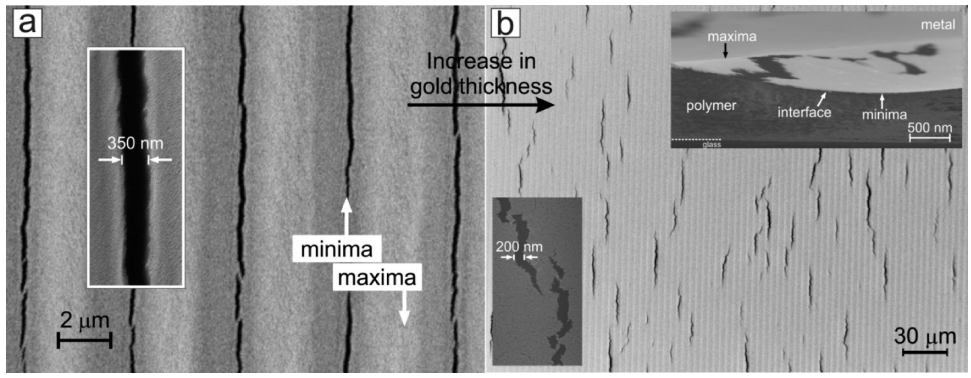

Figure 3. (a) SEM image of a 15 nm thick gold film ruptured during SRG formation. The position of the cracks relative to the topography maxima and minima is marked by the white arrows. (b) SEM image of a 25 nm thick gold layer ruptured during SRG formation. In the right upper corner, a SEM micrograph of the side view of a glass/polymer/metal sample is inserted. The inserts in both micrographs show cracks of 350 and 200 nm width for a 15 and 25 nm thick gold layer, respectively.

Zigzag cracks appear at the maximum of each grating line on the polymer topography and have characteristic orientations at angles between 50° and 60° to a grating vector. In the valleys, the cracks are confined along a line perpendicular to the grating vector. The width differs as well, to be larger (up to 400 nm) at maximum of the SRG. This indicates that different kinds of stresses and strains are acting on the gold film, and may at some point give a valuable hint how forces within the polymer layer are generated.

It is well-known that the process of gold deposition (physical vapor deposition or sputtering) significantly alters the film quality and thus the mechanical response due to residual stress.[35] In our experiments, we tested metal films deposited by both of the above-mentioned methods and observed no significant contribution of residual stresses for crack formation. Similar cracks appeared for these metal films (different evaporation processes) under constant experimental parameters such as intensity, interference pattern (±45), thickness of the metal and polymer layers and irradiation time. We also analyzed any possible contribution of heat generated at the metal/polymer interface during long time exposure to light, causing rupture of metal films due to thermal expansion coefficient mismatch. Our experiments are performed in laboratory atmosphere that ensures a constant temperature around the sample of roughly 20 °C. At the sample surface we have stable interfering beams of 20 mW power. Measurements showed about a loss of 10% after transmission through the sample. We also measured that most of the light that is not transmitted is reflected by the glass/polymer/metal interfaces. So the actual sample material absorbs roughly 1% of the incoming light amounting to 0.2 mW. Assuming an air layer of 1 mm thickness, above the sample surface, we can calculate the heat being conducted away from the sample based up on the Fourier law: $\Delta Q = k(A)/(b)\Delta T$, where, k is heat conductivity of air = 0.024 W/mK, A is the contact area = 0.3 cm^2, b is the distance over which the heat needs to be transferred, and ΔT is a temperature difference of 10 K, which we chose arbitrarily as a realistic value that is well below glass-transition temperature of PAZO. Using these values, we determined a possible heat transfer from the sample of 7.2 mW. Comparing to the input of 0.2 mW, we can exclude significant rise in temperature.

However, the process of gold deformation and the development of cracks depend strongly on the thickness of the gold layer. The periodic rupturing occurs up to a layer thickness of 15 nm although the diagonal crack pattern at the topography maxima are increasingly suppressed as the metal thickness grows (Figure 3a), while the cracks at the minima become more pronounced. Even for much thicker films cracks occur, though not evenly spaced, as can be inferred from the SEM micrographs of a 25 nm Au film (Figure 3b) ruptured irregularly. Similar cracks were observed for a thickness of up to 60 nm. The crack runs vertically through the whole metal film as it can be seen from the cross-sectional AFM analysis (Figure 3b). The characteristic crack observed here is similar to the results reported previously[36] for cracking a 100 nm thin metal film adhered to the polymer substrate. However, the mechanism of stress applied here is completely different, as the polymer film was exposed to a tensile stress.

We should emphasize that at this stage of investigation, we can only speculate about the mechanisms of crack formation and rupture. We may of course use standard models that are frequently employed in material science to estimate the stresses that the polymer exerts on the metal film. In fact, there are plenty of fundamental studies on the deformation and stability of hybrid materials consisting of metal film deposited on a flexible polymer substrate, as it is of fundamental importance for industrial applications such as flexible electronics. A mechanism of fast fracture would imply that the elastic energy stored in the deformed metal sheet is released into the formation of cracks.[37] According to this approach the stress needed to form a crack is $\sigma = ((EG_c)/(\pi a))^{1/2} \approx 0.4$GPa, where E, G_c, $(EG_c)^{1/2}$, and a are the Young modulus, toughness, fracture toughness, and crack length, respectively. For a typical value of fracture toughness of gold thin films[38] $(EG_c)^{1/2} = 0.7$ MN/m$^{3/2}$ and a crack length of 1.0 ± 0.1 μm as measured from SEM images, the stress exerted from the photosensitive polymer film on a gold layer evaluates to ∼0.4 ± 0.1 GPa. On the other hand, one might apply a model frequently used for metal laminated polymer substrates that are put under tensile strain. In this model, transverse cracks form by a local rupturing of the metal sheet as a result of necking, i.e., local thinning.[39] From a standard equation: $\sigma = K\varepsilon^N$, we may estimate local stress to be $\sigma = 0.1$ GPa. Here we use values for the strain, $\varepsilon = 0.024$ calculated as described above; for the prefactor, $K = 114$ MPa and the hardening exponent, $N = 0.02$, which are typical for a weakly hardening metal.[40]

The phenomenon reported in this study should be much more complicated to model because in contrast to a global transverse load the strains in our system occur locally as can be seen from the different shape and size of the cracks formed at

the valleys and ridges of the polymer topography. Also, bending of the metal film and thus its stiffness should play a role. However, even the rough estimations put forward above give reasonable values of the stresses exerted by the polymer on the adsorbed metal film during mass transport. These values are in the range of several hundreds of MPa, and are in good agreement with the theoretically predicted stress.[27] The forces inscribing a topographical pattern into a thin film are hard to assess experimentally and this work could be a starting point for the use of thin metal films to probe and characterize the extent and strength of material flow locally.

CONCLUSION

In this paper we discuss the mechanical forces that arise during irradiation of azo-benzene containing photosensitive polymer films. It was shown that the flow of polymer material in these films can exert significant stresses on adsorbed metal films resulting in the formation of elongated cracks. We have found that the rupturing occurs regularly along maxima and minima of polymer topography up to the metal thickness of around 15 nm. For higher values of the thickness, cracking still takes places but the process is no longer homogeneous along the extrema of the topography, resulting in randomly distributed cracks. The shape and size of the cracks varies depending on whether they occur at the maxima or minima of the polymer topography, clearly indicating local variations of the strain and stress within the polymer film.

Summarizing, in this paper, we have suggested that the response of a metal layer on top of photosensitive polymer upon deformation of the latter might constitute a test of the forces generated within the polymer film. In combination with suitable simulations combining continuum mechanics with molecular dynamics, this might be developed into a method to probe and quantify forces developed during the mass transport of the photosensitive polymer films on molecular scales. In particular, we might ultimately address the question how a polymer film in its glassy state can deform so drastically without significant softening, at the same time doing significant work rupturing the adsorbed metal film.

AUTHOR INFORMATION

Corresponding Author

*E-mail: santer@uni-potsdam.de.

Notes

The authors declare no competing financial interest.

ACKNOWLEDGMENTS

The work is supported by the priority program SPP-1369, DFG, and Volkswagen Stifftung, Germany. We thank Dr. Lasar Kulikovski for the inevitable discussions and fruitful ideas.

REFERENCES

(1) Rochon, P.; Batalla, E.; Natansohn, A. *Appl. Phys. Lett.* **1995**, *66*, 136−138.
(2) Kim, D. Y.; Tripathy, S. K.; Li, L.; Kumar, J. *Appl. Phys. Lett.* **1995**, *66*, 1166−1168.
(3) Rau, H. *Photochemistry and Photophysics*; CRC Press: Boca Rotan, FL, 1990; Vol. *II*, pp 119−141.
(4) Todorov, T.; Nikolova, L.; Tomova, N. *Appl. Opt.* **1984**, *23*, 4309−4312.
(5) Jones, C.; Day, S. *Nature* **1991**, *351*, 15.
(6) Loucif-Saibi, R.; Nakatani, K.; Delaire, J. A.; Dumont, M.; Sekkat, Z. *Chem. Mater.* **1993**, *5*, 229−236.
(7) Sekkat, Z.; Knoll, W., Eds. *Photoreactive Organic Thin Films*; Academic Press: San Diego, CA, 2002, p 399−427.
(8) Eich, M.; Wendorff, J. H. *Makromol. Chem., Rapid Commun.* **1987**, *8*, 467−471.
(9) Todorov, T.; Nikolova, L.; Tomova, N. *Appl. Opt.* **1984**, *23*, 4588−4591.
(10) Todorov, T.; Nikolova, L.; Stoyanova, K.; Tomova, N. *Appl. Opt.* **1985**, *24*, 785−788.
(11) Kim, D. Y.; Li, L.; Jiang, X. L.; Shivshankar, V.; Kumar, J.; Tripathy, S. K. *Macromolecules* **1995**, *28*, 8835−8839.
(12) Barrett, C. J.; Natansohn, A. L.; Rochon, P. L. *J. Phys. Chem.* **1996**, *100*, 8836−8842.
(13) Lefin, P.; Fiorini, C.; Nunzi, J. M. *Opt. Mater.* **1998**, *9*, 323−328.
(14) Bellini, B.; Ackermann, J.; Klein, H.; Grave, C.; Dumas, P.; Safarov, V. *J. Phys.: Condens. Matter.* **2006**, *18*, S1817−S1835.
(15) Seki, T. *Bull. Chem. Soc. Jpn.* **2007**, *80*, 2084−2109.
(16) Natansohn, A.; Rochon, P. *Chem. Rev.* **2002**, *102*, 4139−4175.
(17) Yager, K. G.; Barrett, C. J. *Soft Mater.* **2007**, *3*, 1249−1261.
(18) Ichimura, K. *Chem. Rev.* **2000**, *100*, 1847−1873.
(19) Yager, K. G.; Barrett, C. J. *J. Photochem. Photobiol. A: Chem.* **2006**, *182*, 250−261.
(20) Yager, K. G.; Barrett, C. J. *Curr. Opin. Solid State Mater. Sci.* **2001**, *5*, 487−494.
(21) Ichimura, K.; Oh, S. K.; Nakagawa, M. *Science* **2000**, *288*, 1624−1626.
(22) Finkelmann, H.; Nishikawa, E.; Pereira, G. G.; Warner, M. *Phys. Rev. Lett.* **2001**, *87*, 015501.
(23) Yu, Y.; Nakano, M.; Ikeda, T. *Nature* **2003**, *425*, 145−146.
(24) Ferri, V.; Elbing, M.; Pace, G.; Dickey, D. M.; Zharnikov, P. S.; Mayor, M.; Rampi, M. A. *Angew. Chem., Int. Ed.* **2008**, *47*, 3407−340.
(25) François, D.; Pineau, A.; Zaoui, A. *Mechanical Behaviour of Materials: Vol. II: Viscoplasticity, Damage, Fracture, and Contact Mechanics*; Springer: New York, 1998.
(26) Toshchevikov, V.; Saphiannikova, M.; Heinrich, G. *J. Phys. Chem. B* **2009**, *113*, 5032−5045.
(27) Veer, P. U.; Pietsch, U.; Rochon, P.; Saphiannikova, M. *Mol. Cryst. Liq. Cryst.* **2008**, *486*, 1108−1120.
(28) Saphiannikova, M.; Neher, D. *J. Phys. Chem. B* **2005**, *109*, 19428−19436.
(29) Karageorgiev, P.; Neher, D.; Schulz, B.; Stiller, B.; Pietsch, U.; Giersig, M.; Brehmer, L. *Nat. Mater.* **2005**, *4*, 699−703.
(30) Schuh, C.; Lomadze, N.; Kopyshev, A.; Rühe, J.; Santer, S. *J. Phys. Chem. B* **2011**, *115*, 10431−10438.
(31) Lomadze, N.; Kopyshev, A.; Ruhe, J.; Santer, S. *Macromolecules* **2011**, *44*, 7372−7377.
(32) Private discussion with Prof. Christopher Barrett.
(33) Goldenberg, L. M.; Kulikovska, O.; Stumpe, J. *Langmuir* **2005**, *21*, 4794−4796.
(34) Yadavalli, N. S.; Santer, S. *J. Appl. Phys.* **2013**, *113*, 224304.
(35) Thornton, J. A.; Hoffman, D. W. *Thin Solid Films* **1989**, *171*, 5−31.
(36) Xiang, Y.; Li, T.; Suo, Z.; Vlassak, J. J. *Appl. Phys. Lett.* **2005**, *87*, 161910.
(37) Anderson, T. L. *Fracture Mechanics: Fundamentals and Applications*; CRC Press: Boca Raton, FL, 2005, 31−96.
(38) Olliges, S.; Gruber, P. A.; Orso, S.; Auzelyte, V.; Ekinci, Y.; Solak, H. H.; Spolenak, R. *Scr. Mater.* **2008**, *58*, 175.
(39) Li, T.; Huang, Z. Y.; Xi, Z. C.; Lacour, S. P.; Wagner, S.; Suo, Z. *Mech. Mater.* **2005**, *37*, 261−273.
(40) Li, T.; Suo, Z. *Int. J. Solids Struct.* **2006**, *43*, 2351−2363.